J|A|C|S ARTICLES

Published on Web 11/13/2009

Plasmonic Split-Ring Resonators as Dichroic Nanophotonic DNA Biosensors

Alasdair W. Clark, Andrew Glidle, David R. S. Cumming, and Jonathan M. Cooper*

Department of Electronics and Electrical Engineering, University of Glasgow, Rankine Building, Oakfield Avenue, Glasgow, U.K., G12 8LT

Received July 22, 2009; E-mail: j.cooper@elec.gla.ac.uk; aclark@elec.gla.ac.uk

Abstract: Surface enhanced resonance Raman spectroscopy (SERRS) is a powerful molecular sensing tool that can be applied to a number of applications in the field of molecular diagnostics. We demonstrate that by using electron beam lithography to manipulate the nanoscale geometry of Ag split-ring resonators we can tune their optical properties such that they exhibit two independently addressable high frequency plasmon resonance modes for SERRS. This tailored multimodal, polarization dependent activity enables the split rings to act as discriminating sensors, with each resonance tuned for a particular sensing purpose. The structures are used as multiwavelength, multianalyte DNA SERRS sensors, with each resonance tuned to both the absorption wavelength of a differently colored Raman reporter molecule and its corresponding laser excitation wavelength. The ability of each resonance to independently sense small concentrations of a single DNA type from within a mixed population is demonstrated. Also shown is the effect of the split ring's dichroic response on the SERRS signal and the sensor's limit of detection of each resonance mode (switching its sensory reaction "on" and "off" depending on the orientation of the exciting light).

Introduction

The inherent plasmonic properties of metallic nanoparticles can provide ultrasensitive biosensing platforms based upon Raman spectroscopy.[1] Resonant enhancement of the structure's free electron oscillations by external radiation amplifies the local electromagnetic field around such nanoparticles, facilitating surface enhanced Raman scattering (SERS) from molecules on or near the nanostructure's surface. SERS is a powerful analytical tool whose sensitivity can compete with fluorescence when combined with the resonance Raman effect (SERRS), a technique which has enabled single molecule detection.[1] Furthermore, the structural information afforded by Raman spectroscopy, based upon the vibrational modes of the molecular bond composition, enables multiplexed identification of specific molecular fingerprints. These features make SERRS an ideal tool for molecular diagnostic assays. Here we show that by engineering the multimodal plasmon resonances in single-geometry nano-split-ring-resonator arrays, we can fabricate highly functional nanophotonic DNA biosensors with targeted dichroic properties. By tuning these nanostructures to exhibit two independently addressable plasmon resonances for SERRS, we show each resonance can be used for tailored, multiplexed biosensing to detect low levels of specific DNA sequences from within a mixture of oligonucleotides.

Electron beam lithography has enabled a new generation of optically active nanostructures with defined geometries and plasmonic characteristics to be created. Among the more interesting of these new structures are nano-split-ring resonators.[2−4] These highly tunable, multimodal devices have stimulated interest in a range of nano-optical applications, including metamaterial generation and biosensing.[5,6] The ability to tune the ring's higher order modes to wavelengths within the visible spectrum, along with the strong, predictable, and well dispersed nature of their localized plasmon, makes such structures ideal candidates for surface enhanced resonance Raman scattering (SERRS).

SERRS relies on the frequency of both the exciting radiation and the particle plasmon matching the electronic absorption of the analyte. Control of the nature of a nanoparticle's plasmon resonances, by engineering of the nanostructure's geometry, is therefore essential for the development of new, highly functional photonic biosensors. Many nanostructured substrates described in SERS have used either aggregations of colloidal particulates[7] or simple engineering of noncomplex geometries.[8] However, these approaches can restrict the functionality of the sensor as it is difficult to create particles with multimodal optical properties or, particularly in the case of colloidal aggregates, accurately control the magnitude and location of their electromagnetic hot spots. In addition, poor geometric constraint and/

(1) Nie, S. M.; Emory, S. R. *Science* **1997**, *275* (5303), 1102–1106.
(2) Clark, A. W.; Sheridan, A. K.; Glidle, A.; Cumming, D. R. S.; Cooper, J. M. *Appl. Phys. Lett.* **2007**, *91* (9), 093109.
(3) Rockstuhl, C.; Lederer, F.; Etrich, C.; Zentgraf, T.; Kuhl, J.; Giessen, H. *Optics Express* **2006**, *14* (19), 8827–8836.
(4) Rockstuhl, C.; Zentgraf, T.; Guo, H.; Liu, N.; Etrich, C.; Loa, I.; Syassen, K.; Kuhl, J.; Lederer, F.; Giessen, H. *Appl. Phys. B* **2006**, *84* (1−2), 219–227.
(5) Linden, S.; Enkrich, C.; Wegener, M.; Zhou, J. F.; Koschny, T.; Soukoulis, C. M. *Science* **2004**, *306* (5700), 1351–1353.
(6) Liu, G. L.; Long, Y. T.; Choi, Y.; Kang, T.; Lee, L. P. *Nat. Methods* **2007**, *4* (12), 1015–1017.
(7) Zhu, Z. H.; Zhu, T.; Liu, Z. F. *Nanotechnology* **2004**, *15* (3), 357–364.
(8) Gunnarsson, L.; Bjerneld, E. J.; Xu, H.; Petronis, S.; Kasemo, B.; Kall, M. *Appl. Phys. Lett.* **2001**, *78* (6), 802–804.

10.1021/ja905910q CCC: $40.75

or periodicity of the nanoparticles can lead to spectral broadening and diminish the resonance Raman scatter from those structures with peak wavelengths shifted from that of the laser. As an alternative to such colloidal systems, structures including nonsymmetrical particles or coupled particle pairs, which exhibit distinct resonances at different polarization angles, have been shown to produce multiple high frequency resonances and have the potential to be employed as multifunctional sensors.[8−11] However, due to the weakness of the resonances in these simple nonsymmetrical particles,[9,10] and the greatly increased plasmonic damping seen in coupled particle pairs,[11] the multiple resonances are not ideal for independent SERRS use.

In this paper, we propose an alternative paradigm, involving the engineering of a split-ring nanostructure's geometry to precisely control both the number and nature of plasmon resonances generated, matching them to the electronic absorptions of already synthesized Raman reporter molecules. Significantly, this allows us to exploit the SERRS effect (which can provide enhancements several orders of magnitude greater than SERS) at two distinct wavelengths for an array of geometrically defined nanophotonic structures. This greatly increases the functionality of the device when compared to structures with single resonance peaks, enhancing the sensitivity of the device at these wavelengths as well as enabling multiplexing, as molecules labeled with a variety of existing Raman-active labels can be detected with equal fidelity at appropriate absorption wavelengths (avoiding the need for the excessive spectral deconvolution that would be required were a single resonance peak be used for SERRS of several molecules).

Although dual wavelength SERRS DNA assays have been performed using aggregations of colloidal metals,[12] an engineered array of plasmonic structures with multiple resonance modes, as is presented in this paper, ensures predictable, reproducible electric field enhancements around specific facets of the structure's geometry for each resonance, a feature not provided by a randomly aggregated colloid. Electron beam lithographic fabrication of Ag nano split-ring resonators allows us not only to tune the number of optical resonance modes but also the wavelength, magnitude, and physical location of the resonantly induced electromagnetic field for each mode. Ensuring the SERRS signal is maximized for each laser wavelength and without having to rely on the randomly distributed field enhancements of a colloidal aggregation. This direct-write fabrication technique enables highly functional, highly sensitive, multiwavelength DNA sensors based on SERRS that can be engineered to operate at different wavelengths pertaining to different applications. We show these structures are capable of selective, independent detection of two differently labeled oligonucleotides (ODNs) hybridized against complementary strands, immobilized on the silver sensor surface using SERRS. The polarization dependence of the nanoparticle's plasmon creates a sensory dichroism with "on" and "off" states defined at two chosen wavelengths.

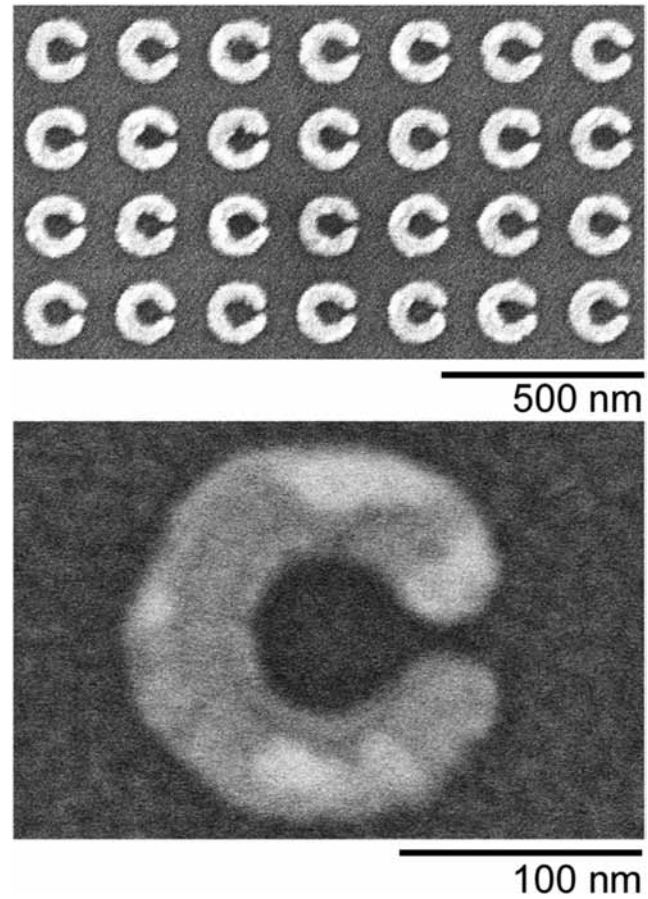

Figure 1. SEM of a split-ring array showing a high level of array uniformity (top). Individual structure (bottom). The pattern was written into a PMMA, poly(methylmethacrylate), resist bilayer on a 500 μm thick Pyrex substrate, using a Vistec VB6 UHR EWF electron beam writer; we used thermal evaporation of metal (using an in-house evaporator) followed by acetone lift-off to fabricate the array of Ag split-ring structures. Uniformity of device dimensions across the arrays was measured as 79 $\pm$ 2 nm for the radius, 49 $\pm$ 3 nm for the wall thickness, and 10 $\pm$ 2 for the gap size (measured from a sample of 10 structures). Plasmonic characterization of the ring arrays was performed using a Shimadzu UV3101PC absorption spectrometer. A self-assembling monolayer (SAM) of 3-aminopropyltriethoxysilane was used to ensure good adhesion of the 20 nm Ag layer to the substrate.

Results and Discussion

The Ag nano split-ring arrays were fabricated on 500 μm thick Pyrex substrates using a combination of electron-beam lithography and resistive heating evaporation. Figure 1 shows a high resolution SEM of a fabricated split-ring array. The design of these structures was informed by finite difference time domain (FDTD) modeling, which, combined with strict uniformity of their manufacture across Figure 1, ensured that the multiple, polarization dependent resonances were strong, sharp, and closely spaced (Figure 2). By appropriate choice of dimensions and metallization, we tuned the dichroic resonances to 785 nm and 633 nm (wavelengths corresponding to electronic resonances associated with Cy5 and Cy7). Choosing electron beam lithography as a fabrication technique allowed us to precisely control the dimensions of the rings while providing an excellent level of array homogeneity, ensuring the plasmonic response over the entire sample is identical and delivering good sample-to-sample reproducibility.

Figure 2 shows the plasmonic peak spectra of the split-ring array when light was polarized both parallel and perpendicular

(9) Félidj, N.; Grand, J.; Laurent, G.; Aubard, J.; Lévi, G.; Hohenau, A.; Galler, N.; Aussenegg, F. R.; Krenn, J. R. *J. Chem. Phys.* **2008**, *128* (9), 094702.
(10) Payne, E. K.; Shuford, K. L.; Park, S.; Schatz, G. C.; Mirkin, C. A. *J. Phys. Chem. B* **2006**, *110* (5), 2150–2154.
(11) Rechberger, W.; Hohenau, A.; Leitner, A.; Krenn, J. R.; Lamprecht, B.; Aussenegg, F. R. *Opt. Commun.* **2003**, *220* (1−3), 137–141.
(12) Faulds, K.; McKenzie, F.; Smith, W. E.; Graham, D. *Angew. Chem., Int. Ed.* **2007**, *46* (11), 1829–1831.

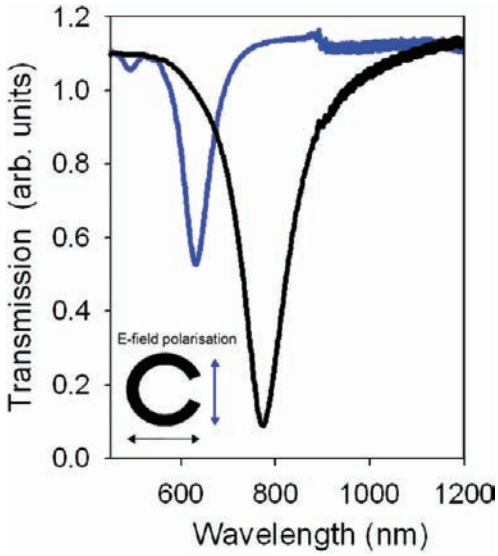

Figure 2. Multimodal plasmonic resonances of 80 nm radius Ag split-ring and typical plasmonic activity of the Ag split-ring resonator arrays when the electric field is polarized perpendicular and parallel to the split in the ring geometry. The average peak resonance wavelengths across identical arrays were well-defined, measured as 772 ± 14 nm for the $N = 2$ resonance and 631 ± 3 nm for the $N = 3$ resonance. A thin film linear polarizer controlled the electric field vector of the incident light beam, and each array was measured with the electric field polarized both perpendicular and parallel with respect to the split in the ring geometry; see inset.

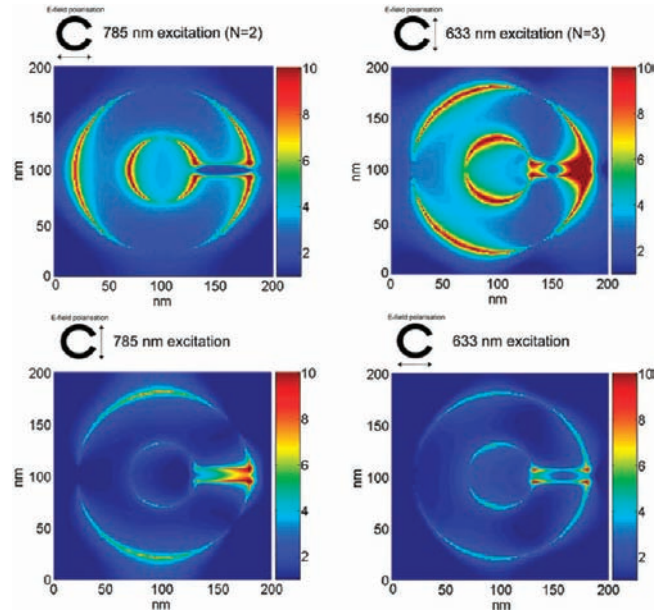

Figure 3. Graphical representation of the nanostructure's field activity when the electric field of the incident light is polarized parallel and perpendicular to the split in the ring geometry. Finite difference time domain simulations were performed at the two excitation wavelengths (~633 and ~785 nm) showing the "on" and "off" sensor states at different polarizations.

to the gap. Plasmonic characterization of the ring arrays was performed using a Shimadzu UV3101PC absorption spectrometer. A Thor Laboratories linear thin film polarizer controlled the electric field vector of the incident light beam, and each array was measured with the electric field polarized both perpendicular and parallel with respect to the split in the ring geometry. Nanocrescent split-ring resonators of this size will support up to three polarization dependent resonances, two resonances when the electromagnetic field is parallel to the gap, and one when it is perpendicular to the gap ($N = 1$, 2, and 3, denoting the first, second, and third order resonances).[2,13,14] As can be seen in Figure 2, these resonances are sufficiently well-defined to provide the necessary molecular specificity. Despite being only 150 nm apart they do not overlap significantly and maintain their polarization independence. FDTD modeling was not only used to inform the fabrication but also to obtain a graphical representation of the localized electric field activity around the structures at each of the resonance wavelengths, Figure 3. This allowed us to determine which areas of the ring provide the greatest proportion of the overall Raman scattered signal. Consistent with Figure 2, this activity shows greater amplitude and more widespread distribution across the structure when the incident electric field is polarized to excite the individual resonance (the sensory "on" state). Although there was some localized enhancement in the "off" state it was not nearly as pronounced, clearly demonstrating the advantage of the individual resonance peaks (noting in particular the weak field seen for the "off" state of $N = 3$, even though Figure 2 shows this to overlap with the trailing edge of $N = 2$).

Target ODN sequences, 3′-modified with a thiol group (TGCAGATAGATAGCAGT3-SH), were adsorbed onto the split-ring array. The coverage of this initial layer on the individual rings was assumed to be approximately 30 pmol cm^{-2}, matching that of similarly sized sequences found in the literature.[15] Competitive hybridization assays between two complementary probe sequences, 5′-modified with Raman active cyanine dyes Cy5 and Cy7 respectively, were then performed. The choice of sequence modification ensured that, following hybridization, the cyanine dyes were located proximal to the silver surface, maximizing both SERRS signal and the fluorescence quenching. Raman measurements were carried out using a Horiba Jobin Yvon LabRam INV spectrometer in conjunction with 0.5 mW 633 nm HeNe laser and 9.5 mW 785 nm diode laser excitation sources. Data were collected when the electric field vector of each laser was orientated both parallel and perpendicular to the split in the ring geometry, the separate plasmonic states generated by turning the sample through 90° with respect to the polarization of the laser source to give "on" and "off" resonance conditions predicted by simulation, Figure 3, and shown in Figures 2 and 4. Each Raman measurement was performed in triplicate, and the mean value used.

Figure 4 shows the Raman scattered signal for a competitive assay resulting from complementary binding from an equimolar concentration of Cy5−2CTGCTATCTATCTGCA and Cy7−2CTGCTATCTATCTGCA (the concentration of each was 250 μM). Although their molecular structure is similar, the SERRS spectra of Cy5 and Cy7 possess unique vibrational bands that allow their identification (namely 1189 cm^{-1} for Cy5 and 1135 cm^{-1} for Cy7).[16−19] Whilst it is possible to detect unlabeled DNA strands using Raman scattering, the addition of a label

(13) Clark, A. W.; Glidle, A.; Cumming, D. R. S.; Cooper, J. M. *Appl. Phys. Lett.* **2008**, *93* (2), 023121.
(14) Sheridan, A. K.; Clark, A. W.; Glidle, A.; Cooper, J. M.; Cumming, D. R. S. *Appl. Phys. Lett.* **2007**, *90* (14), 143105.
(15) Vidal, B. C.; Deivaraj, T. C.; Yang, J.; Too, H. P.; Chow, G. M.; Gan, L. M.; Lee, J. Y. *New J. Chem.* **2005**, *29* (6), 812–816.
(16) Sato, H.; Kawasaki, M.; Kasatani, K.; Katsumata, M. A. *J. Raman Spectrosc.* **1988**, *19* (2), 129–132.
(17) Stokes, R. J.; Macaskill, A.; Lundahl, P. J.; Smith, W. E.; Faulds, K.; Graham, D. *Small* **2007**, *3* (9), 1593–1601.
(18) Yang, J. P.; Callender, R. H. *J. Raman Spectrosc.* **1985**, *16* (5), 319–321.

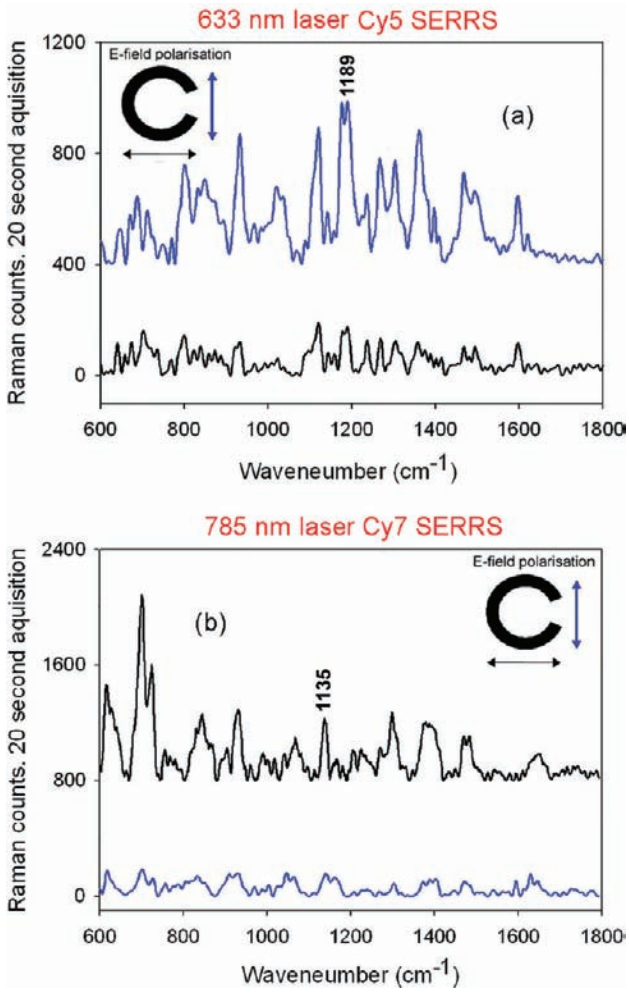

Figure 4. SERRS from an array modified with sequences of Cy5 and Cy7 labeled oligonucleotide sequences hybridized to a thiolated oligonucleotide strand. Measurements were performed at 633 and 785 nm, and data were collected when the electric field vector of each laser was both (a) parallel ($N = 3$ resonance, Cy5-ODN, 633 nm) and (b) perpendicular ($N = 2$ resonance, Cy7-ODN, 785 nm) to the split in the ring geometry. Spectra have undergone background correction. All measurements were performed in triplicate, and mean responses were used. The very weak SERRS signals in the "off" resonance state (Figure 4, and in our simulations, Figure 2) are due to either the lightning rod effect from the particle's areas of high curvature[20,21] or contributions from chemical enhancement (charge transfer) effects.[22,23] Control experiments using labeled noncomplementary ODN show zero Raman scattering confirming that SERRS is provided solely by hybridized strands and that nonspecific binding is minimal and does not influence the SERRS signal.

with a distinctive Raman fingerprint allows individual sequences to be identified. Furthermore, the signal enhancement provided by the SERRS effect increases the Raman scatter, and therefore the sensitivity of the technique, by several orders of magnitude. For each laser, the SERRS signal (the Raman scattering from the colored tag molecules associated with the excitation

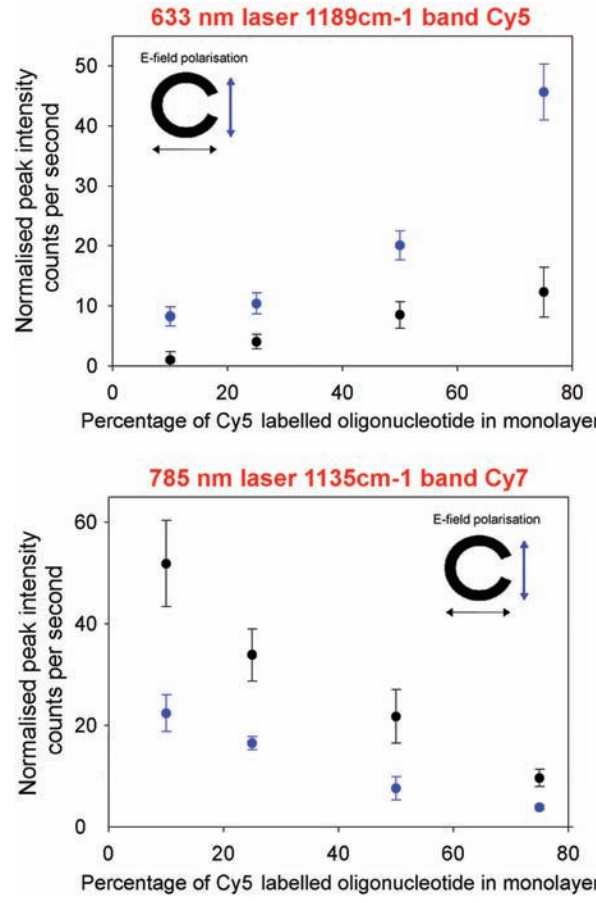

Figure 5. Peak intensities of Raman spectra collected from arrays of Ag split rings modified with varying ratios of the two sequences. Excitation was at 633 and 785 nm.

wavelength) greatly dominates the fluorescence from the associated tag, as well as the nonresonant Raman (SERS) signals from the dye not associated with the excitation source: using the 633 nm laser, Raman scattering (SERRS) from the Cy5 labeled sequence only was detected. By rotating the sample through 90° the Cy5 signal is turned "off" and the resonance associated with 785 nm can be used to detect SERRS from the Cy7 labeled ODN, once again without interference from the Cy5 labeled sequences. When the device is rotated to its "off" position, for either excitation wavelength, there is a significant drop in Raman scattering due to the disappearance of the plasmonic resonance at these polarizations (~4× for $N = 3$, ~6× for $N = 2$).

The presence of strong plasmonic resonances at $N = 2$ and $N = 3$ becomes particularly important as the quantity of the target molecule is reduced. ODN mixtures containing different ratios of the Cy5 and Cy7 sequences were hybridized against a number of separate arrays, modified with complementary strands, leading to each array being covered by a mixed monolayer with a different ratio of the two dyes, Figure 5. Initially a target ODN sequence, (TGCAGATA-GATAGCAGT3-SH) 3′-modified with a thiol group was adsorbed to the Ag surface. Competitive hybridization assays between two complementary Raman active 5′-labeled ODN probe sequences (namely Cy5−2CTGCTATCTATCTGCA and Cy7−2CTGCTATCTATCTGCA) were carried out. In all assays the total concentration of ODN mixture was constant at 250 μM. As the percentage of the Cy5 labeled

(19) Stokes, R. J.; Macaskill, A.; Dougan, J. A.; Hargreaves, P. G.; Stanford, H. M.; Smith, W. E.; Faulds, K.; Graham, D. *Chem. Commun.* **2007**, (27), 2811–2813.
(20) Crozier, K. B.; Sundaramurthy, A.; Kino, G. S.; Quate, C. F. *J. Appl. Phys.* **2003**, *94* (7), 4632–4642.
(21) Sherry, L. J.; Chang, S. H.; Schatz, G. C.; Van Duyne, R. P.; Wiley, B. J.; Xia, Y. N. *Nano Lett.* **2005**, *5* (10), 2034–2038.
(22) Campion, A.; Kambhampati, P. *Chem. Soc. Rev.* **1998**, *27* (4), 241–250.
(23) Otto, A. *J. Raman Spectrosc.* **2005**, *36* (6−7), 497–509.

sequence was increased, the intensity of the Raman scattered Cy5 signal from the $N = 3$ resonance also increased, whilst that for the Cy7 signal matched to the $N = 2$ resonance decreased. As the relative concentration of either labeled sequence was lowered, the Raman signal from the "off"-resonance states become indistinguishable from the background, demonstrating that in such low concentration conditions (10% surface coverage for the $N = 3$ mode, 25% surface coverage for the $N = 2$ mode) the structures act as dichroic sensory switches at two independent wavelengths.

The resonance Raman signals dominate at each wavelength. Even for 75% coverage of either sequence, no bands other than those produced by the SERRS effect are detected; i.e. only Cy5 is detected at 633 nm and only Cy7 at 785 nm, regardless of field orientation. With this in mind, and taking into account the data seen in this figure, it would be possible to estimate the relative coverage of each sequence on the sensor if presented with an unknown mixture.

Figure 3 informs us that only a fraction of the silver surface is involved with plasmon generation.[13] Despite this, and assuming a surface area of approximately 1.68×10^{-10} cm^2 per ring and literature values for surface coverage of ligand,[15] the limit of detection corresponds to ~500 molecules per element for the $N = 3$ mode and ~1250 molecules per element for the $N = 2$ mode, with the number of sensing elements contributing to the spectra (those illuminated by the focused laser spot) expected to be 12 and 16 respectively. The probability is, however, that the signal is being generated by a smaller number of individual molecules situated within the plasmonic hot spots illustrated in Figure 3; hence only a fraction of the molecule numbers quoted above will actually be contributing to the SERRS signal.

Finally, it was noted that the $N = 2$ resonance was less sensitive (in that it had a higher limit of detection) than the $N = 3$ resonance. This phenomenon results not only as a consequence of the strength of the resonance and the distribution of its associated field enhancement but also due to the fact that the efficiency of the Raman scattering is related to the wavelength of the exciting light by $1/\lambda^4$.

Conclusion

In conclusion, we have demonstrated that the multiple plasmonic resonances of nanophotonic split-ring particle arrays can be tuned to create unique dichroic biosensors based on SERRS. We demonstrate that by engineering a single nanostructure's geometry we can control the number and nature of its multimodal plasmon resonances, matching these to the electronic absorptions of multiple labels. This allows us to exploit the SERRS effect at two separate wavelengths in a controlled, reproducible fashion, providing a new paradigm in the functionality of engineered plasmonic substrates, as well as that of multiplexed SERRS biosensing.

Acknowledgment. The authors would like to thank the RASOR interdisciplinary research collaboration initiative, BBSRC, EPSRC, Scottish Funding Council, for funding of this research.

Supporting Information Available: The Supporting Information describes the experimental procedures used, including fabrication protocols, simulation parameters, DNA binding and hybridization protocols, Raman instrumentation details, and data acquisition and processing information. This information is available free of charge via the Internet at http://pubs.acs.org.

JA905910Q